Macromolecules

Article

pubs.acs.org/Macromolecules

Ionic Transport, Microphase Separation, and Polymer Relaxation in Poly(propylene glycol) and Lithium Perchlorate Mixtures

Fei Fan,[†] Yangyang Wang,*[,‡] and Alexei P. Sokolov[†,‡]

[†]Department of Chemistry, University of Tennessee, Knoxville, Tennessee, 37996, United States

[‡]Chemical Sciences Division, Oak Ridge National Laboratory, Oak Ridge, Tennessee, 37831, United States

Supporting Information

ABSTRACT: By combining broadband dielectric spectroscopy (BDS) and differential scanning calorimetry (DSC), the ionic transport, microphase separation, and polymer relaxation in poly(propylene glycol) (PPG) and lithium perchlorate ($LiClO_4$) mixtures have been systematically examined as a function of temperature, pressure, polymer molecular weight, and salt concentration. While the low molecular weight PPG–$LiClO_4$ mixtures exhibit only a single phase, microphase separation is observed in the mixtures of higher molecular weight PPGs (1000 and 4000 g/mol). In the samples with microphase separation, BDS and DSC yield consistent glass transition temperatures for ion-rich and ion-depleted domains. Our Walden plot analysis indicates that the ionic transport in PPG–$LiClO_4$ is controlled by the (slow) segmental relaxation, and the data of all PPG–$LiClO_4$ fall close to the "ideal" Walden line. Last, the application of pressure not only suppresses the microphase separation, but also decouples the ionic transport from the segmental relaxation.

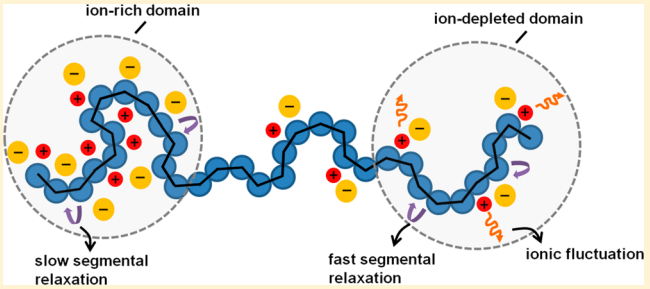

1. INTRODUCTION

A significant amount of effort has been put into the study of solid polymer electrolytes because of their advantages over the traditional liquid electrolytes and potential applications in energy storage and electrochemical devices.[1−4] However, the mechanism of ion transport in the polymer electrolytes has not been completely understood, which has impeded the development of novel materials with desired ionic conductivity. None of the current dry polymer electrolytes can exhibit conductivity greater than 10^{-3} S cm^{-1} at ambient temperature.

Poly(ethylene oxide) (PEO) and poly(propylene glycol) (PPG) were first recognized as promising candidates for polymer electrolytes in the 1970s,[5−7] and since then have been studied intensively due to their high ability to solvate salts and low glass transition temperatures.[1,8−17] PEO is prone to form crystalline phase with most of the salts, which makes it an unsatisfactory system for the study of ion transport mechanism.[18−20] To avoid this difficulty, low molecular weight PPGs are typically chosen as an alternative system for polymer electrolytes related fundamental studies. Unfortunately, it has been shown, by several different experimental techniques, that the overall amorphous PPG–salt complexes exhibit microphase separation over a wide salt concentration range.[21−23,16] Differential scanning calorimetry (DSC) studies from Vachon et al. showed two glass transition temperatures (T_gs) in several PPG–salt complexes.[21,23] It was proposed that ion-rich and ion-depleted phases were formed as a result of the competition between the Li–O binding energy and the long-range Coulombic interactions. Additionally, two segmental relaxations were observed in the dielectric spectroscopy study of PPG–$LiClO_4$,[16] as well as the study of PPG–$NaCF_3SO_3$ by photon correlation spectroscopy.[22]

Furthermore, microphase separation has been found in several other polymer electrolytes. For example, Yoshida et al. reported a split of segmental relaxation in PEO–$LiClO_4$ in its amorphous phase.[17] Zhang and Runt also observed similar behavior in poly(vinyl methyl ether) (PVME)–$LiClO_4$.[24] All these findings suggest that microphase separation might widely exist in dry polymer electrolytes, and a systematic experimental study to clarify its physical origin and influence on the ionic transport, therefore, seems necessary. In addition, the molecular weight of many novel ionic conducting polymers is typically on the order of a few kilograms per mole.[25] In this limit, both molecular weight[26] and terminal groups[27,28] may play an important role in the ionic transport properties of the polymer. A thorough understanding of low molecular weight PPG can serve as the next step toward a complete elucidation of microphase separation and ion transport in solid polymer electrolytes in general.

Pressure is an important experimental variable that strongly influences the dynamics and thermodynamics of glass-forming liquids and polymers. While the dielectric behavior of neat PPG under high pressure has been extensively studied,[29−33,28] much less attention has been given to PPG-based electrolytes, i.e.,

Received: June 15, 2013
Revised: November 17, 2013
Published: November 22, 2013

   dx.doi.org/10.1021/ma401238k | Macromolecules 2013, 46, 9380−9389

PPG−salt mixtures. The existing high-pressure studies are primarily focused on the conductivity aspect,[34−36] little is known about the influence of pressure on microphase separation and relaxation of PPG with salts.

Here, we present a detailed analysis of the dielectric behavior of PPG-based electrolytes, by systematically varying the experimental temperature, pressure, polymer molecular weight, and salt concentration. Microphase separation has been observed by both differential scanning calorimetry (PPG4000−$LiClO_4$, O:Li = 10, 15) and dielectric spectroscopy (PPG4000−$LiClO_4$, O:Li = 1000, 30, 15, 10; PPG1000−$LiClO_4$, O:Li = 30) in some of the samples. Our analysis indicates that both the polymer molecular weight and the number of terminal hydroxyl groups contribute to the different thermal and dielectric behavior of PPG−$LiClO_4$. Using a modified Walden plot analysis, we demonstrate that the ionic conductivity is controlled by the slow segmental relaxation in samples with microphase separation. Regardless of microphase separation, all the PPG data from (slow) segmental relaxation fall close to the "ideal" Walden line, exhibiting apparent similarity to other systems with ionic conductivity strongly coupled to structural relaxation, such as aprotic ionic liquids and salt aqueous solutions. In addition, we have carried out dielectric spectroscopy measurements under high pressure. The degree of microphase separation is found to decrease with increase of pressure. Most importantly, the close relationship between ionic transport and segmental relaxation breaks down at sufficiently high pressure, where the sample (PPG4000−$LiClO_4$, O:Li = 30) starts to resemble superionic conductors. To the best of our knowledge, this is the first time such an effect has been observed for polymer electrolytes.

2. MATERIALS AND METHODS

2.1. Materials. Poly(propylene glycol) (PPG) of 425 and 1000 g/mol were purchased from Sigma-Aldrich and PPG of 4000 g/mol was obtained from Scientific Polymer Products. Lithium perchlorate ($LiClO_4$) was purchased from Alfa Aesar. All materials were used as received. The polymers and salts were first dissolved in methanol and then mixed in proportions to achieve desired concentration of salt. The concentration was represented by the molar ratio of ether oxygen to lithium (O:Li) and samples with O:Li = 1000, 30, 15, 10, and 7 were made. To remove methanol, the samples were placed under high vacuum at room temperature for more than 4 weeks and then at 80 °C for 12 h. All the samples were optically clear.

2.2. Differential Scanning Calorimetry (DSC). The samples for DSC measurements were sealed in aluminum hermetic pans. A TA thermal instrument Q1000 was used to record the heat flow. The measurements were performed from 70 °C and cooled to −90 °C and then heated back to 70 °C. The cooling and heating rates were 10 °C/min. Each cooling and heating scan was repeated several times to make sure that the results were reproducible. The glass transition temperature (T_g) was taken as the midpoint of the step in the heat flow in the cooling process. The high T_g in PPG4000−$LiClO_4$ (O:Li = 15) and the low T_g in PPG4000−$LiClO_4$ (O:Li = 10) could not be accurately determined from the conventional DSC, because of the relatively small heat flow change involved. As a result, temperature-modulated DSC was used for these two samples. The scan started at +40 °C and ended at −90 °C, with ramp rate of 3 °C/min, modulation amplitude of 1 °C, and modulation period of 60 s.

2.3. Broadband Dielectric Spectroscopy (BDS). Broadband dielectric measurements were performed in the frequency range of 10^{-2}−10^7 Hz, using a Novocontrol Concept 80 system, which includes an Alpha-A impedance analyzer, a ZGS active sample cell interface, and a Quatro Cryosystem temperature control unit. The samples were placed between two gold-plated electrodes separated by a Teflon spacer. The experiments proceeded from high to low temperatures. The samples were equilibrated at each temperature for 10−20 min before the dielectric measurements.

The high-pressure dielectric measurements were carried out in a Unipress high pressure system with a parallel capacitor. The Alpha-A analyzer was connected to the dielectric cell through a ZG4 interface. The temperature was controlled by the PRESTO system from Julabo.

3. RESULTS

3.1. Differential Scanning Calorimetry. Representative heat flow curves from DSC measurements are presented in Figure 1. Only a single T_g can be observed at low and high salt concentrations, while two T_gs are found in PPG4000−$LiClO_4$ at intermediate concentration (O:Li = 15 and 10). The observation of two T_gs in PPG4000−$LiClO_4$ is consistent with the earlier DSC studies.[21,23] For all three molecular weights, the glass transition temperature of PPG−$LiClO_4$ increases with the increase of salt concentration. For example, the T_gs of PPG425−LiClO4 at O:Li = 1000, 15, and 7 are 196 K, 212 and 229 K, respectively. It is worth noting that while the three neat PPGs (425, 1000, and 4000) have similar T_gs, the T_g of PPG−$LiClO_4$ exhibits clear molecular weight dependence (e.g., Figure 1 bottom panel). A complete summary of the concentration and molecular weight dependence of T_g in PPG−$LiClO_4$ is presented in Figure 11.

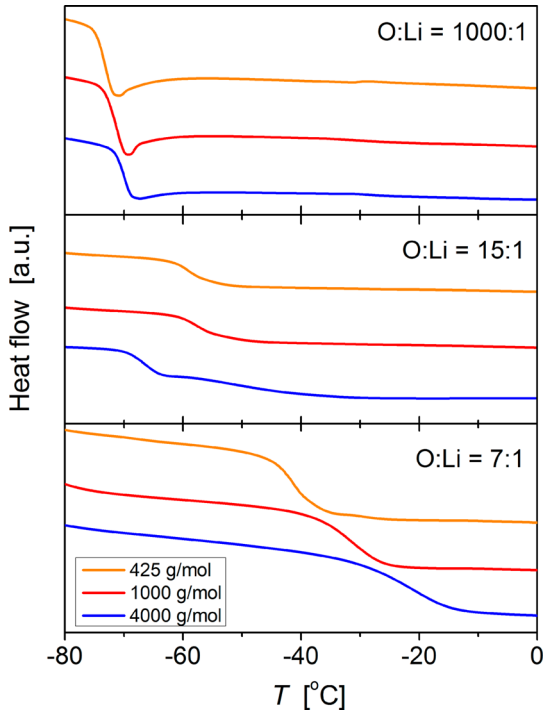

Figure 1. DSC curves recorded at the heating process on PPG−$LiClO_4$ complexes: (a) O:Li = 1000:1 (low concentration of $LiClO_4$), (b) O:Li = 15:1 (intermediate concentration), and (c) O:Li = 7:1 (high concentration). Orange (top), red (middle), and blue (bottom) curves stand for 425, 1000, and 4000 g/mol, respectively. The data for PPG4000−$LiClO_4$ (O:Li = 15) is from the irreversible heat flow in the temperature-modulated DSC measurement.

3.2. Broadband Dielectric Spectroscopy. *3.2.1. Spectra Analysis.* Representative dielectric spectra of $\varepsilon'(f)$, $\varepsilon''(f)$ and derivative $\varepsilon''_{der}(f)$ [$\varepsilon''_{der} = (-\pi/2)\partial\varepsilon'/\partial(\ln f)$] of PPG−$LiClO_4$ are shown in Figure 2. They consist of three major components: (1) slow and fast segmental relaxations in the high-frequency region; (2) dc conductivity in the midfrequency

dx.doi.org/10.1021/ma401238k | Macromolecules 2013, 46, 9380−9389

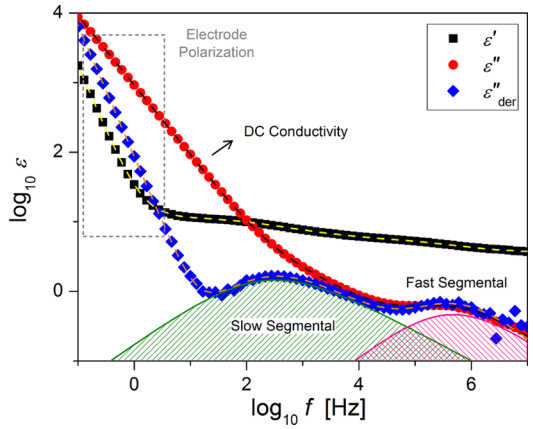

Figure 2. Dielectric spectrum of PPG4000–$LiClO_4$ (O:Li = 30) at −30 °C. There are three major components: (1) split of the segmental relaxations (fast and slow) in the high-frequency region, (2) dc conductivity in the intermediate-frequency region of ε'', and (3) the sharp increase of ε' and ε''_{der} in the low-frequency region due to the electrode polarization effect. Solid symbols represent the experiment results and the dashed lines represent the fits.

region of $\varepsilon''(f)$; and (3) sharp increase of $\varepsilon'(f)$ and ε''_{der} in the low-frequency region due to the electrode polarization (EP) effect. It should be emphasized that the purpose of presenting Figure 2 is to demonstrate the general fitting procedure of the spectra, whereas the actual number of relaxation processes may vary, depending on the polymer molecular weight, salt concentration, temperature and pressure (see the Discussion below).

The complex permittivity spectra can be fit by the superposition of several functions, including Havriliak–Negami equations,[37] a dc conductivity term, and an electrode polarization term:

$$\varepsilon^*(\omega) = \varepsilon_\infty + \sum_j \frac{\Delta\varepsilon_j}{[1 + (i\omega\tau_{HN,j})^{\alpha_j}]^{\beta_j}} + \frac{\sigma}{i\varepsilon_0\omega} + A\omega^{-n} \quad (1)$$

Here, $\omega = 2\pi f$ is the angular frequency, ε_∞ represents the value of $\varepsilon'(\omega)$ at infinite frequency, $\Delta\varepsilon_j$ is the dielectric relaxation strength, $\tau_{HN,j}$ is the relaxation time, α_j, β_j are the shape parameters of process j, n gives the slope of EP's high frequency tail, A is related to the amplitude of EP, and σ is the dc conductivity. The conductivity obtained from the fitting procedure is essentially identical to that from direct reading of $\sigma'(\omega)$ in the dc plateau region. In this study, the frequency at ε'' maximum is used to calculate the relaxation time (τ_{max}). The τ_{max} is related to the Havriliak–Negami relaxation time τ_{HN}, and shape parameters α and β by the following equation:[37]

$$\tau_{max} = \tau_{HN}\left(\sin\frac{\alpha\beta\pi}{2+2\beta}\right)^{1/\alpha}\left(\sin\frac{\alpha\pi}{2+2\beta}\right)^{-1/\alpha} \quad (2)$$

The analysis of the dielectric spectra of polymer electrolytes is often plagued by the high level of ionic conductivity. Multiple relaxation processes might be completely masked by the dc conductivity in $\varepsilon''(\omega)$. In this study, we use the derivative spectra (e.g., Figure 2, blue diamonds), $\varepsilon''_{der} = (-\pi/2)\partial\varepsilon'/\partial(\ln\omega)$, based on the Kramers–Kronig relations, to assist our data analysis.[38,24] On the one hand, the derivative spectra are used to determine the number of relaxation processes and therefore the number of fitting terms in eq 1. On the other hand, they are used to check the quality of the fit of $\varepsilon'(\omega)$. In most cases, the use of derivative spectra significantly improves the accuracy of the analysis.

3.2.2. General Features of the Dielectric Spectra of PPG–$LiClO_4$. The dielectric spectra of all the neat PPGs and the PPG–$LiClO_4$ complexes are shown in Figure 3. The dielectric relaxation in neat PPG has been the subject of many studies.[39−42,37,43,30,44,26,28] It is well-known that two relaxations in general can be observed in PPG: a segmental relaxation at high frequencies, and a slower "normal mode" at low frequencies, which is due to the relaxation of the end-to-end vector of the entire polymer chain. In the neat PPG425 (Figure 3a–c), only the segmental relaxation is visible, because of the relative short length of this polymer. In the neat PPG1000 (Figure 3d–f), the normal mode appears as a weak shoulder close to the segmental peak. In the neat PPG4000 (Figure 3g–i), the normal mode becomes more separated from the segmental relaxation.

The addition of $LiClO_4$ salt shifts the segmental relaxation to lower frequencies (Figure 3). At low salt concentration (O:Li = 1000), a new process ("ionic mode") appears in all three PPG–$LiClO_4$ complexes. In PPG4000–$LiClO_4$ (O:Li = 1000, 30, 15, 10) and PPG1000–$LiClO_4$ (O:Li = 30), a split of segmental relaxation into fast and slow processes can be observed. It can

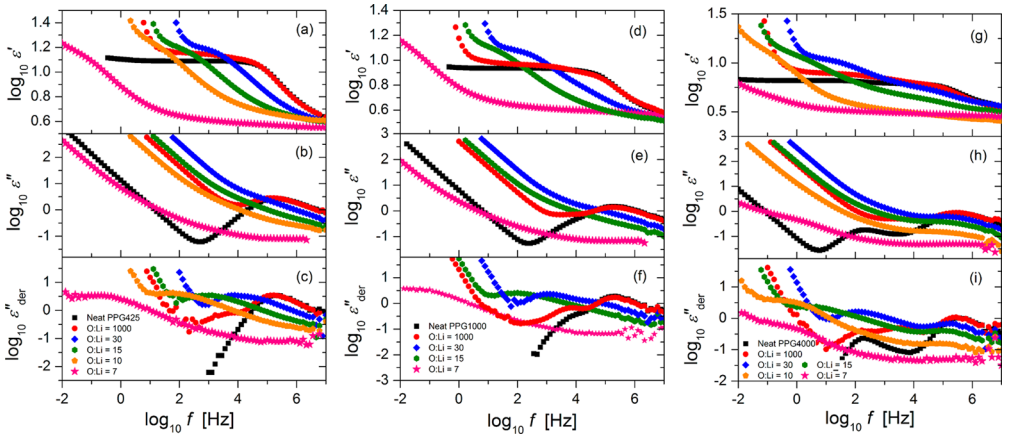

Figure 3. Comparison of the dielectric spectra of neat PPG and PPG/$LiClO_4$ with different molecular weight: (a–c) 425 g/mol at −36 °C; (d–f) 1000 g/mol at −35 °C; (g–i) 4000 g/mol at −34 °C.

dx.doi.org/10.1021/ma401238k | Macromolecules 2013, 46, 9380–9389

also be seen from Figure 3 that with the addition of salt, the ionic conductivity starts to interfere with the polymer relaxation. Not only the segmental relaxation is eventually covered by ionic conductivity in $\varepsilon''(f)$, but also the EP starts to influence $\varepsilon'(f)$ at high salt concentrations.

3.2.3. Spectra at Low Salt Concentration. While only the segmental relaxation is visible in the neat PPG425, an additional relaxation shows up at low frequencies in PPG425−$LiClO_4$ (O:Li = 1000) due to the presence of $LiClO_4$ (Figure 3a−c, Figure 4a). Similar processes are also

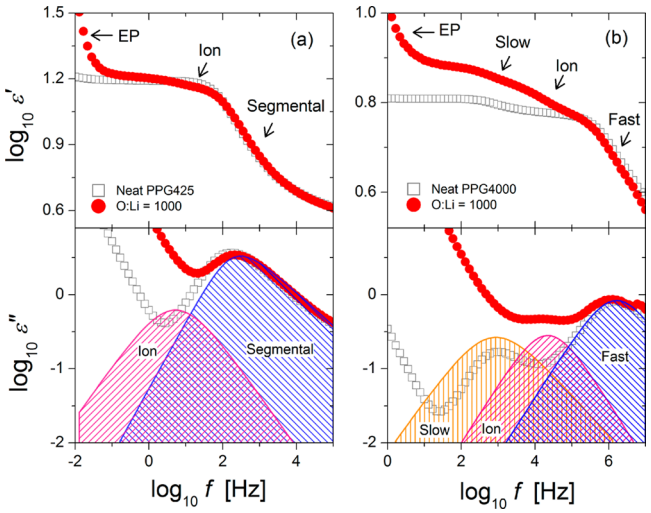

Figure 4. Comparison of the dielectric spectra of PPG (a) 425 and (b) 4000 g/mol at O:Li = 1000 (low salt concentration). The open squares present the spectra of neat polymers and the closed circles present the spectra of PPG−$LiClO_4$. The peaks represent different relaxation processes from the fitting of PPG−$LiClO_4$ spectra. The increase of ε' at low frequencies is due to the electrode polarization effect (EP).

found in PPG1000−$LiClO_4$ (O:Li = 1000) (Figure 3d−f) and PPG4000−$LiClO_4$ (O:Li = 1000) (Figure 3g−i, Figure 4b). This relaxation is assigned as "ionic mode" (see discussions in section 4.1).

In PPG4000−$LiClO_4$ (O:Li = 1000), a slow process appears at almost the same position as the normal mode in neat PPG4000 (Figure 4b), although with increased relaxation strength. This mode is assigned as slow segmental relaxation (see discussions in section 4.2). At O:Li = 1000:1, although the slow segmental mode in PPG4000 appears at the frequency of normal mode in neat PPG, this seems to be a coincidence. We have determined the chain relaxation times of PPG-based electrolytes using rheological measurements. In general, the chain relaxation times from rheology and the slow segmental relaxation times from dielectric spectroscopy do not coincide (see Supporting Information for details). In PPG1000−$LiClO_4$ (O:Li = 1000), two processes are clearly observable (Figure 3d-f). They are ionic mode and fast segmental mode. Because of the presence of the ionic mode, it is hard to resolve the slow segmental peak from the spectrum. The fast segmental processes in PPG4000−$LiClO_4$, PPG1000−$LiClO_4$ at O:Li = 1000, as well as the only segmental process in PPG425−$LiClO_4$ at O:Li = 1000, do not differ much from the segmental peaks in the corresponding neat PPGs, in terms of both peak frequency and shape.

3.2.4. Spectra at Intermediate Salt Concentration. At intermediate salt concentration, the spectra of PPG4000−$LiClO_4$ become considerably different from that of the neat PPG4000 (Figure 3g−i). The split of segmental relaxation is much more pronounced (Figure 5b). With the increase of salt

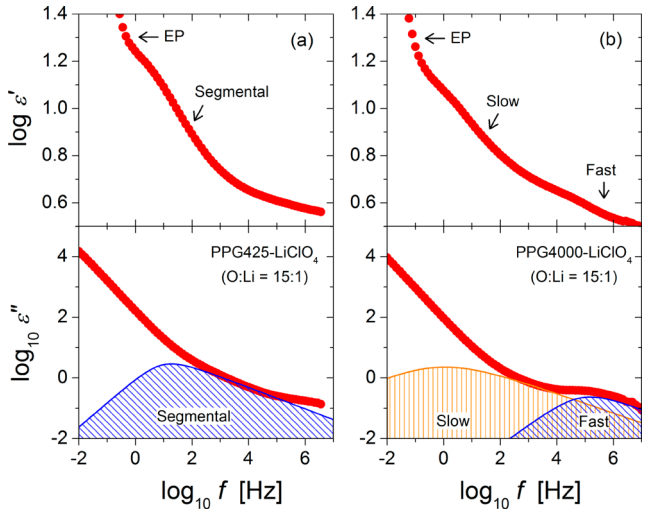

Figure 5. Comparison of the dielectric spectra of PPG−$LiClO_4$ with molecular weight (a) 425 and (b) 4000 g/mol at O:Li = 15:1 (intermediate salt concentration). The peaks represent different relaxation processes from the fitting of the spectra.

concentration, the relaxation strength of the slow process increases, while the strength of the fast process is reduced, and becomes unobservable when O:Li = 7 (Figure 6). It should be

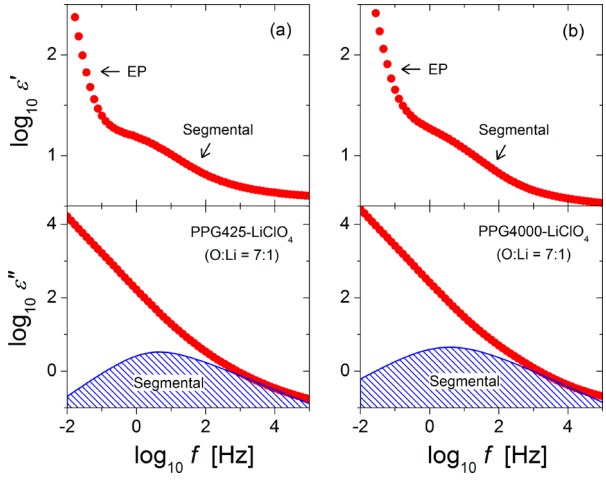

Figure 6. Comparison of the dielectric spectra of PPG−$LiClO_4$ with molecular weight (a) 425 and (b) 4000 g/mol at O:Li = 7:1 (high salt concentration).

noted that the separation between slow and fast segmental relaxations also becomes larger with the increase of $LiClO_4$ concentration (Figure 3g−i). It is also worth pointing out that the slow relaxation is qualitatively different from the low-frequency artifact that is frequently observed in viscous liquids.[45,46] The presence of impurities such as air bubbles often leads to an ultraslow Debye-like relaxation. In contrast, the slow (segmental) relaxation in PPG−$LiClO_4$ is much broader, especially at high salt concentrations. In addition, the

dx.doi.org/10.1021/ma401238k | Macromolecules 2013, 46, 9380−9389

agreement between the results of BDS and DSC clearly indicates that the origin of the slow dielectric peak is the segmental relaxation of the polymer in the ion-rich domain (see section 4.2).

In PPG1000−$LiClO_4$, as the salt content increases to O:Li = 30, the ionic mode is no longer observable and the segmental relaxation splits into two separate processes (Figure 3d−f), similar to the behavior of PPG4000−$LiClO_4$. The fast segmental relaxation becomes unobservable when O:Li ≤ 15.

In PPG425−$LiClO_4$, with the increase in salt concentration the segmental relaxation process shifts to lower frequencies (Figure 3a−c, 5a). No splitting of segmental process is observed in the concentration range studied.

3.2.5. Spectra at High Salt Concentration. At high salt concentration (O:Li = 7), only a single segmental relaxation peak, with shape much broader than the original segmental peak in the neat PPG, is observed in all three PPG−$LiClO_4$ mixtures (Figure 3 and 6). This result is consistent with the DSC measurement where only one T_g is detected at O:Li = 7.

4. DISCUSSION

4.1. Nature of the Ionic Mode. *4.1.1. Molecular Weight, Temperature, and Concentration Dependence.* At O:Li = 1000, a new relaxation process appears on the low-frequency side of the (fast) segmental relaxation in PPG−$LiClO_4$ of all three molecular weights (Figures 3 and 4). This mode becomes unobservable when O:Li ≤ 30. The relaxation strength and relaxation time of this new mode and segmental mode are presented as a function of reciprocal temperature in Figure 7. It

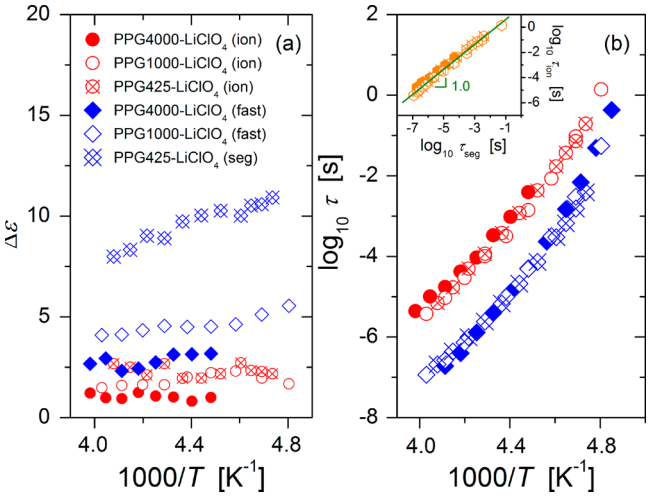

Figure 7. Temperature dependence of (a) the relaxation strength and (b) relaxation time for the fast segmental and ion modes. The red circles and blue diamonds represent the ionic mode and segmental mode, respectively. Inset: relation between the ionic and segmental relaxation times. The filled, open, and crossed symbols correspond to PPG4000, PPG1000, and PPG425, respectively.

can be seen that in the entire temperature range of this study, (1) the relaxation strength of the new (ionic) mode does not significantly depend on the molecular weight of PPG while the relaxation strength of the segmental mode decreases with increase of the molecular weight of PPG; (2) the relaxation time of both the new (ionic) mode and segmental mode is almost independent of the molecular weight of PPG. The same additional relaxation (ionic mode) was also observed in PPG−$LiClO_4$ by Furukawa et al.[15,16] They showed that the strength of this mode increased with increasing salt concentration in the range of 100 ≤ O: Li ≤ 1000. Furthermore, the inset of Figure 7 indicates that the ionic mode closely follows the (fast) segmental relaxation; i.e., they have similar temperature dependence. Runt et al. observed a similar ionic mode in PEO-based single-ion conductors.[47] Because the lithium ion interacts more strongly with the polyether backbone than the perchlorate ion does, this ionic mode might resemble the counterion fluctuations in polyelectrolyte solutions,[48] where the polarization caused by the mobile ion fluctuation gives rise to the change of dielectric permittivity. In other words, on short time scale, the slower lithium cations might "stick" to the polymer backbone, with faster perchlorate anions "floating" around, analogous to polyelectrolytes.[49,50] As we demonstrate below, the slow and fast relaxations originate from the segmental relaxations in ion-rich and ion-depleted domains, respectively. Since the ionic mode is slower than the fast segmental relaxation, but faster than the slow segmental relaxation, it should only arise from the ion fluctuation in the ion-depleted domain. However, the exact nature of the ionic mode requires further investigation.

4.1.2. Ionic Mode under High Pressure. The dielectric spectra of PPG425−$LiClO_4$ (O:Li = 1000) at ambient and high pressure (551 MPa) are shown in Figure 8. The strength and

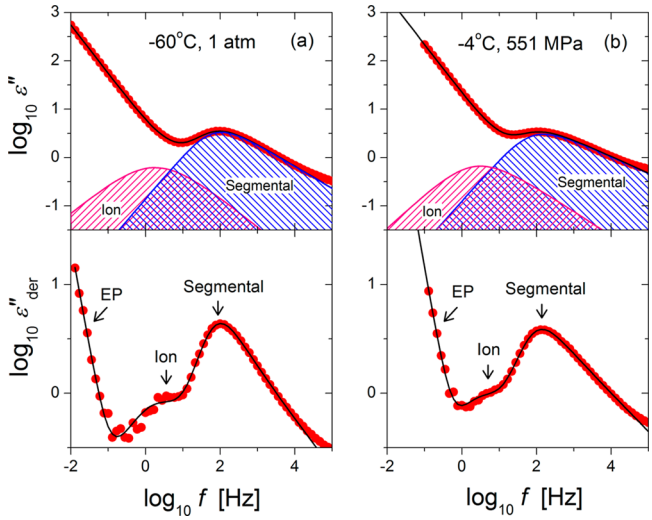

Figure 8. Comparison of the spectra of PPG425−$LiClO_4$ (O:Li = 1000) at (a) ambient pressure (1 atm) and (b) high pressure (551 MPa).

shape of the ionic and segmental relaxation at the two pressures are almost identical, despite a slight decoupling of ionic conductivity from the segmental relaxation at high pressure. The relaxation times of the ionic and segmental modes are presented as a function of pressure in Figure 9. Similar to the effect of decrease of temperature, the increase of pressure shifts the ionic and segmental modes to lower frequencies. The inset shows the relation of the ionic relaxation to the segmental relaxation under both isothermal and isobaric conditions. The data fall onto the same line of a slope of one, indicating that the ionic and segmental modes are affected in a very similar fashion by pressure and temperature. Moreover, the inset suggests that these two modes are well coupled at the studied pressure and temperature range.

4.2. Origin of the Slow and Fast Relaxations. *4.2.1. Correlation between BDS and DSC.* Two (segmental)

dx.doi.org/10.1021/ma401238k | Macromolecules 2013, 46, 9380−9389

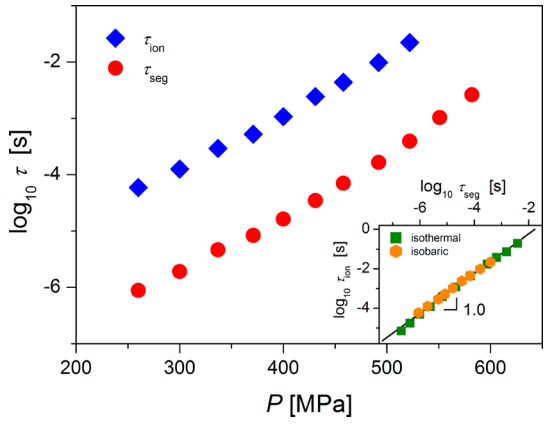

Figure 9. Relaxation time as a function of pressure for both ion mode (diamonds) and segmental mode (circles). The inset shows the relationship between the relaxation time of the ion mode and the segmental mode in isothermal (squares) and isobaric (hexagons) experiments.

relaxations (slow and fast) are observed in PPG4000−$LiClO_4$ (O:Li = 1000, 30, 15, 10) and PPG1000−$LiClO_4$ (O:Li = 30). This is presumably related to the well-known microphase separation behavior in PPG-based electrolytes.[21−23,16] However, the results of dynamic and calorimetric measurements have never been directly compared. In our dielectric spectroscopy (BDS) measurements, the temperature dependence of segmental relaxation time (τ) across the temperature range of study can be well described by the Vogel−Fulcher−Tammann (VFT) equation (Figure 10):

$$\tau = \tau_0 \exp[B/(T - T_0)] \quad (3)$$

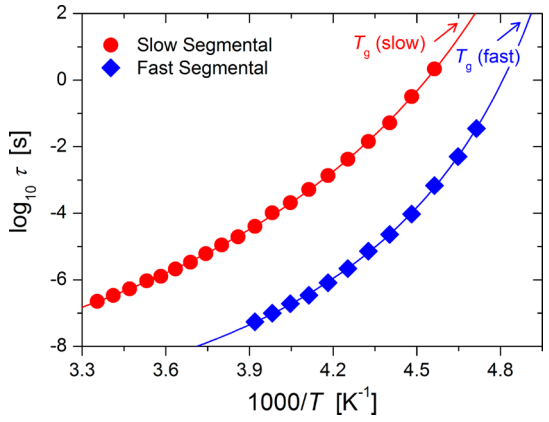

Figure 10. Temperature dependence of slow and fast segmental relaxation times in PPG4000−$LiClO_4$ (O:Li = 30). The solid lines are the fits by eq 3

where τ_0, B, T_0 are the fitting parameters. The glass transition temperature can be defined as the temperature where τ = 100 s. In samples (PPG1000−$LiClO_4$, O:Li = 30 and PPG4000−$LiClO_4$, O:Li = 1000, 30, 15, 10) with the splitting feature, two glass transition temperatures can be obtained using this method (Figure 11). The VFT fit parameters for all the samples are summarized in Table 1−3. The VFT extrapolation of the segmental relaxation time to τ = 100s brings very small error bar to the estimates of T_g due to narrow temperature range of the extrapolation. These error-bars are included in Figure 11. On the other hand, the glass transition temperature can be determined from DSC by taking the midpoint of the change of the heat flow (see Section 2.2).

Figure 11 shows that glass transition temperatures from DSC and BDS are in reasonable agreement with each other. In both cases, (1) T_g increases with the increase of salt concentration; and (2) two T_gs are found at intermediate concentrations O:Li = 15−10 for PPG4000−$LiClO_4$. However, since DSC is not as sensitive as broadband dielectric spectroscopy, only one T_g is found in PPG4000−$LiClO_4$ (O:Li = 1000, 30) and PPG1000−$LiClO_4$ (O:Li = 30), whereas two T_gs are obtained from dielectric analysis. Nevertheless, good agreement has been found for DSC and BDS T_gs, wherever a direct comparison is possible. This result confirms that slow and fast relaxations indeed come from the polymer segmental motions in different microdomains. Since it is expected that the ion-polymer interaction would slow down the segmental relaxation, the fast and slow segmental relaxations should correspond to the motions in the ion-depleted and ion-rich domains, respectively.

4.2.2. Effects of Molecular Weight and Terminal Groups. Both DSC and BDS measurements indicate that the glass transition temperature (of either ion-rich or ion-depleted domain) of PPG−$LiClO_4$ increases monotonically with the increase of salt concentration. This is because the transient "cross-linking" between lithium cations and ether oxygens slows down the segmental dynamics of the polymer matrix. The effect of salt on T_g is relatively small at low salt concentration. However, the T_g of PPG−$LiClO_4$ with high salt content is considerably higher than that of the neat PPG. It has been demonstrated that the terminal groups play an important role in the glass transition of low molecular PPGs.[51,28] For example, in the molecular weight range 425−4000 g/mol, the T_g of hydroxyl-terminated PPG varies less than 1%, while the T_g of methyl-terminated PPG strongly depends on the molecular weight.[51] It has been proposed that such a difference is caused by the hydrogen bonding formed by the terminal hydroxyl (OH) groups which reduces the segmental mobility of the polymer. When $LiClO_4$ is added to PPG, the lithium cations prefer to coordinate with the terminal OH groups first,[52] and thus break up the hydrogen bonding between polymer chains. At low salt concentration, there are many unbroken hydrogen bonds, which still strongly influence the glass transition behavior of the samples. The increase of salt content leads to a decrease of hydrogen bonds and an increase of coordination between the OH groups and cations, causing a stronger dependence of T_g on the molecular weight of PPG. Since the

Table 1. VFT Fit Parameters for PPG4000-Based Samples

	PPG4000		O:Li = 1000			O:Li = 30		O:Li = 15		O:Li = 10		O:Li = 7
	chain	segmental	slow	ion	fast	slow	fast	slow	fast	slow	fast	slow
τ_0 [ps]	113	104	119	22.4	0.0291	4.14	1.20	2.93×10^{-3}	4.32	2.94×10^{-3}	12.6	1.67×10^{-3}
B [K]	1206	1079	1211	964.8	1210	1444	827.7	2658	716.2	2321	578.5	2618
T_0 [K]	162.5	168.6	162.8	172.3	166.2	165.5	177.8	152.2	182.1	176	191	177.1

dx.doi.org/10.1021/ma401238k | Macromolecules 2013, 46, 9380−9389

Table 2. VFT Fit Parameters for PPG1000-Based Samples

	PPG1000		O:Li = 1000		O:Li = 30		O:Li = 15	O:Li = 7
	chain	segmental	ion	fast	slow	fast	slow	slow
τ_0 [ps]	0.816	0.199	3.40	0.107	30.4	0.231	1.57×10^{-3}	1.56×10^{-2}
B [K]	1362	1058	1175	1142	960.5	1138	2699	1952
T_0 [K]	157.4	167.9	164.2	165.8	175.6	167.6	148.4	179.1

Table 3. VFT Fit Parameters for PPG425-Based Samples

	PPG425	O:Li = 1000		O:Li = 30	O:Li = 15	O:Li = 10	O:Li = 7
	segmental	ion	segmental	segmental	segmental	segmental	segmental
τ_0 [ps]	0.0129	7.46×10^{-5}	0.0314	0.183	1.56	0.0228	1.54×10^{-3}
B [K]	1527	3011	1387	1424	1103	1689	2306
T_0 [K]	154.3	126.1	156.8	159.8	177.3	170.9	169.4

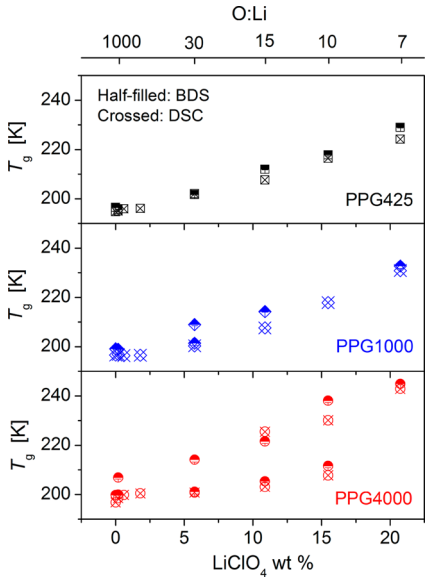

Figure 11. Comparison of the T_gs determined from DSC (crossed symbols) and broadband dielectric spectroscopy (BDS) (half-filled symbols) measurements for the neat PPG and PPG−$LiClO_4$ at various O:Li ratios. The high T_g of PPG4000−$LiClO_4$ (O:Li = 15) and the low T_g of PPG4000−$LiClO_4$ (O:Li = 10) are determined from temperature-modulated DSC measurements, because of the very small change of heat flow in the conventional DSC measurements.

number density of end OH groups increases from PPG4000 to PPG425, the T_g of (the ion-rich domains in) PPG4000−$LiClO_4$ experiences the largest change, whereas the T_g of PPG425−$LiClO_4$ has the smallest change in the studied concentration range.

No microphase separation has been observed in PPG425−$LiClO_4$. In contrast, clear indications of microphase separation are found in PPG4000−$LiClO_4$ (O:Li = 1000, 30, 15, 10) in both DSC and BDS measurements. The polymer molecular weight affects the microphase separation behavior in two ways: (1) the number of repeating units per polymer chain, and (2) the number density of terminal hydroxyl groups. Because the mixing entropy $\Delta S \sim k_B[(1-\phi)\ln(1-\phi) + (\phi/N)\ln\phi]$,[53] with ϕ being the polymer volume fraction and N the number repeating units per chain, the mixtures become less likely to form a homogeneous solution as N increases. In addition, the terminal hydroxyl groups favor the solvation of ions.,[5227] Among the three PPGs in this study, PPG425 has the smallest molecular weight and thus the highest number density of terminal OH groups. As a result, there is no indication of microphase separation for PPG425−$LiClO_4$ in either DSC or BDS measurement. On the other hand, while the split of segmental relaxation is only observed at O:Li = 30 for PPG1000−$LiClO_4$, microphase separation occurs in a much wider concentration range for PPG4000−$LiClO_4$ (O:Li = 1000−10 in BDS; O:Li = 15, 10 in DSC). It is perhaps useful to point out an interesting fact: the fast process in PPG4000−$LiClO_4$ disappears at O:Li = 7, indicating no microphase separation. This O:Li number is the average number of repeating unit in PPG425, in which no microphase separation has been observed at any salt concentration.

4.2.3. Behavior under High Pressure. Pressure is another important parameter that strongly influences the dynamics of polymer electrolytes. As a demonstration, the result of high-pressure dielectric measurement of PPG4000−$LiClO_4$ (O:Li = 30) is shown in Figure 12b, together with the result of isobaric experiments (Figure 12a). With the decrease of temperature or increase of pressure, both slow and fast segmental modes shift to lower frequencies. However, in the isothermal experiments, the two segmental relaxations exhibit different pressure sensitivity. The fast mode shifts quicker than the slow mode

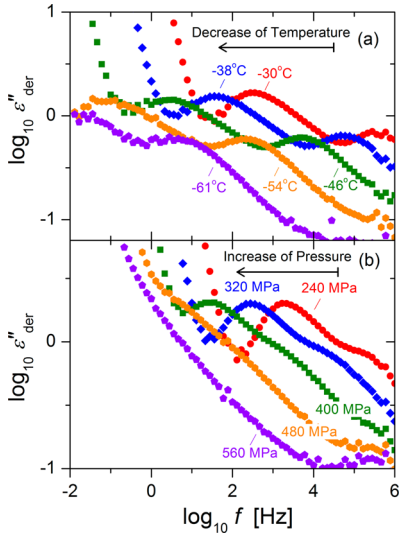

Figure 12. Comparison of the derivative spectra of PPG4000−$LiClO_4$ (O:Li = 30) at (a) various temperatures and (b) pressures. The isobaric measurements (top) were carried out at 1 atm, whereas the isothermal measurements (bottom) were performed at 10.4 °C.

dx.doi.org/10.1021/ma401238k | Macromolecules 2013, 46, 9380−9389

does, and eventually merges into the slow mode as pressure increases, while in the isobaric experiments, both segmental processes show similar sensitivity to the change of temperature. Alternatively, one may interpret this as suppression of microphase separation under high pressure. Because the ion-rich domain might have higher efficiency of packing, the tendency of forming ion-depleted domain decreases under high pressure.

4.3. Relation of Ionic Transport to Segmental Relaxation. *4.3.1. Walden Plot at Ambient Pressure.* According to the classical Walden rule,[54] the molar conductivity (Λ) of many small-molecule electrolytes is inversely proportional to its fluidity ($1/\eta$), here η is viscosity. It is implicitly assumed that all ions are free (complete dissociation) and their diffusion is controlled by the macroscopic viscosity. The Walden rule serves as the basis of a very useful classification of ionic conductors—Walden plot analysis.[13,55−58] In a typical Walden plot analysis, the molar conductivity of a given electrolyte is plotted as a function of its fluidity on double-logarithmic scale. Using a dilute aqueous solution as a reference (e.g., $LiClO_4$), one can draw an "ideal" Walden line with slope of one on the Walden plot (dashed line in Figure 13). This

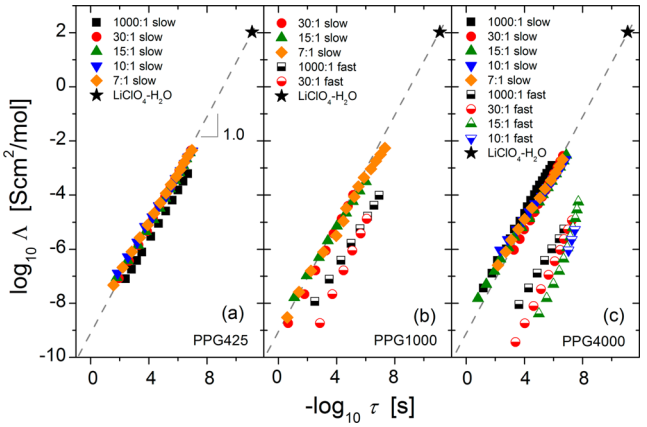

Figure 13. Walden plots for (a) PPG425−$LiClO_4$, (b) PPG1000−$LiClO_4$, and (c) PPG4000−$LiClO_4$. Here, dilute $LiClO_4$ aqueous solution is used as a reference. The dashed line with slope 1.0 is the "ideal" Walden line. For samples with the microphase separation, two groups of data are presented. They are data from the slow segmental mode (closed symbols), and data from the fast segmental mode (semiopen symbols).

"ideal" line divides the plane into superionic (above) and subionic (below) regimes. Two pieces of important information can be obtained from the Walden plot analysis. First, the Walden plot analysis could reveal the degree of coupling or decoupling between ionic transport and structural relaxation. Completely coupled ionic conductors, such as dilute aqueous salt solutions, would show up as a straight line of slope one on the Walden plot. On the other hand, decoupled systems[59−64,25] would display a slope smaller than one. Second, the Walden plot analysis could reveal the intrinsic conducting ability of an ionic conductor relative to the "ideal" aqueous solution. A "good" ionic conductor should appear in the superionic regime of the Walden plot. In polymer electrolytes, the ionic motions are directly related to the local segmental relaxation while macroscopic viscosity is controlled by the chain relaxation. It has been well established that the ionic transport is not controlled by the viscosity of the polymer matrix.[65,66] Experimentally, it has been found that (at a given salt concentration) the ionic conductivities in entangled PEOs are independence of molecular weight,[17] whereas the viscosities strongly depend on the molecule weight as $\eta \sim M^{3.4}$. Therefore, to apply the Walden plot analysis to polymers, the fluidity must be substituted by the rate of structural (segmental) relaxation ($1/\tau$), which is a more relevant quantity for ionic transport in polymers.

The Walden plot for PPG−$LiClO_4$ is shown in Figure 13. Here, it is assumed that all ions are fully dissociated. The dilute $LiClO_4$ aqueous solution is chosen as the reference for constructing the "ideal" Walden line. In PPG425−$LiClO_4$ (Figure 13a), the data of all concentrations fall onto the "ideal" line. In samples with the two segmental modes, PPG1000−$LiClO_4$ (O:Li = 30) (Figure 13b) and PPG4000−$LiClO_4$ (O:Li = 1000, 30, 15, 10) (Figure 13c), the points plotted using the slow segmental relaxation fall close to the "ideal" Walden line, whereas the points plotted using the fast segmental relaxation stay below the "ideal" line. In the rest of the PPG1000−$LiClO_4$ and PPG4000−$LiClO_4$ samples where only a single segmental relaxation is observed, all points fall very close to the "ideal" Walden line as well.

The above Walden plot analysis leads to a clear conclusion: the (slow) segmental relaxation controls the macroscopic ionic conductivity in all the three PPGs regardless of their molecular weight; i.e., the ionic transport in PPG is closely coupled to the (slow) segmental relaxation. In addition, the Walden plot analysis reveals that the ionic mobility of PPG-based electrolytes is very similar to that of the dilute aqueous solutions. The relatively low ionic mobility in PPG at ambient temperature is caused by the slow segmental dynamics, which is additionally slowed down due to the interactions with ions.

4.3.2. Behavior under High Pressure. While the ionic transport in PPG is strongly coupled to the segmental relaxation under ambient pressure, our analysis reveals a different picture at elevated pressures (Figure 14). In PPG4000−$LiClO_4$ (O:Li = 30), the points presented using the slow segmental relaxation fall on the "ideal" Walden line at low pressures (p < 400 MPa), but move into the superionic regime (above the ideal line) when the pressure exceeds 400

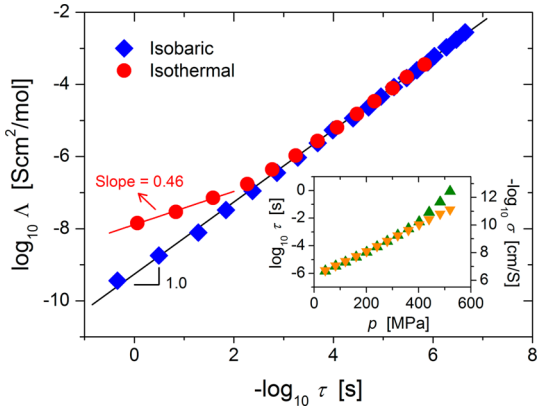

Figure 14. Effects of temperature and pressure on the relationship between ionic transport and (slow) segmental relaxation in PPG4000−$LiClO_4$ (O:Li = 30). The isobaric data (blue diamonds) were obtained by varying temperature at 1 atm. The isothermal data (red circles) were obtained by varying pressure at 10.4 °C. Inset: dependence of the slow segmental relaxation time (green up triangle) and resistivity ($1/\sigma$) (yellow down triangle) on pressure.

dx.doi.org/10.1021/ma401238k | Macromolecules 2013, 46, 9380−9389

MPa. This indicates that at high pressure the ionic motions are decoupled from the segmental relaxation of the polymer. In another words, densification of PPG slows down its segmental dynamics significantly stronger than dynamics of ions. This observation suggests that the close relation between ionic transport and segmental relaxation only holds in a certain pressure range. Because of the asymmetry in size, small ions may require much smaller activation volume for diffusive motion than do the polymer segments. Here, it is important to note that although the electrode polarization (EP) effect interferes the fitting of the dielectric relaxation at high pressures and the obtained segmental relaxation times might be subject to certain error, the overlapping of electrode polarization and segmental relaxation itself is a manifestation of decoupling. This is because EP is controlled by ionic conductivity. If the ionic transport is closely coupled to the segmental relaxation, then the high-frequency tail of EP should move together with the segmental relaxation peak when the pressure is changed. The high-frequency tail of EP and segmental relaxation are well separated at low pressures but strongly overlap at high pressures. This observation indicates that the ionic transport and segmental relaxation are decoupled under high pressure.

5. CONCLUSIONS

Although PPG-based electrolytes have been the subject of many investigations, the present study demonstrates that a complete understanding of these materials cannot be obtained, unless the temperature, pressure, polymer molecular weight, and salt concentration are varied in a systematic manner. Because of the mediocre solvating power of PPG, complex microphase separation behavior shows up in PPGs with relatively high molecular weight. At low salt concentration (O:Li = 1000), an ionic mode has been observed in PPGs of all three molecular weights (425, 1000, and 4000 g/mol). The strength and shape of this ionic relaxation are insensitive to the change of temperature and pressure. Microphase separation is found in PPG4000−$LiClO_4$ (O:Li = 1000, 30, 15, 10) and PPG1000−$LiClO_4$ (O:Li = 30). The T_gs determined for the ion-rich and ion-depleted domains from BDS and DSC are consistent with each other. In contrast to the ionic mode, the microphase separation is strongly suppressed under high pressure. Our Walden plot analysis shows that the ionic transport at ambient pressure in PPG−$LiClO_4$ is controlled by the (slow) segmental relaxation, and all the PPG data fall close to the "ideal" Walden line. These results emphasize the strong coupling of ionic transport to segmental dynamics in PPG-based polymer electrolytes. The reason might be the strong coordination of lithium ions to oxygen atoms in the polymer backbone. However, this close relation between ionic transport and segmental relaxation breaks down at high pressure.

■ ASSOCIATED CONTENT

Supporting Information

Comparison of mechanical and dielectric relaxation times. This material is available free of charge via the Internet at http://pubs.acs.org.

■ AUTHOR INFORMATION

Corresponding Author

*E-mail: (Y.W.) yywang@utk.edu.

Notes

The authors declare no competing financial interest.

■ ACKNOWLEDGMENTS

This research was sponsored by the Laboratory Directed Research and Development Program of Oak Ridge National Laboratory, managed by UT-Battelle, LLC, for the U.S. Department of Energy. F.F. thanks the NSF Polymer Program (DMR-1104824) for funding. The authors are grateful to M. Paluch for the help with the high-pressure dielectric device.

■ REFERENCES

(1) Armand, M. *Solid State Ionics* **1983**, *9−10* (Part 2), 745−754.
(2) Scrosati, B.; Vincent, C. A. *MRS Bull.* **2000**, *25*, 28−30.
(3) Tarascon, J.-M.; Armand, M. *Nature* **2001**, *414*, 359−367.
(4) Wright, P. V. *MRS Bull.* **2002**, *27*, 597−602.
(5) Fenton, D. E.; Parker, J. M.; Wright, P. V. *Polymer* **1973**, *14*, 589.
(6) Wright, P. V. *Br. Polym. J.* **1975**, *7*, 319−327.
(7) Armand, M.; Chabagno, J. M.; Duclot, M. Polyethers as Solid Electrolytes. In *Fast Ion Transport in Solids: Electrodes and Electrolytes*; Vashitshta, P., Mundy, J. N., Shenoy, G. K., Eds.; North Holland Publishers: Amsterdam, 1979.
(8) Watanabe, M.; Ikeda, J.; Shinohara, I. *Polym. J.* **1983**, *15*, 65−69.
(9) Watanabe, M.; Ikeda, J.; Shinohara, I. *Polym. J.* **1983**, *15*, 175−177.
(10) Schantz, S.; Torell, L. M.; Stevens, J. R. *J. Appl. Phys.* **1988**, *64*, 2038−2043.
(11) Schantz, S.; Torell, L. M.; Stevens, J. R. *J. Chem. Phys.* **1991**, *94*, 6862−6867.
(12) Vallée, A.; Besner, S.; Prud'Homme, J. *Electrochim. Acta* **1992**, *37*, 1579−1583.
(13) McLin, M. G.; Angell, C. A. *J. Phys. Chem.* **1996**, *100*, 1181−1188.
(14) Ferry, A.; Orädd, G.; Jacobsson, P. *Macromolecules* **1997**, *30*, 7329−7331.
(15) Kano, K.; Takahashi, Y.; Furukawa, T. *Jpn. J. Appl. Phys.* **2001**, *40*, 3246−3251.
(16) Furukawa, T.; Mukasa, Y.; Suzuki, T.; Kano, K. *J. Polym. Sci., Part B: Polym. Phys.* **2002**, *40*, 613−622.
(17) Yoshida, K.; Manabe, H.; Takahashi, Y.; Furukawa, T. *Electrochim. Acta* **2011**, *57*, 139−146.
(18) Berthier, C.; Gorecki, W.; Minier, M.; Armand, M. B.; Chabagno, J. M.; Rigaud, P. *Solid State Ionics* **1983**, *11*, 91−95.
(19) Scheirs, J.; Bigger, S. W.; Delatycki, O. *Eur. Polym. J.* **1991**, *27*, 1111−1120.
(20) Gadjourova, Z.; Andreev, Y. G.; Tunstall, D. P.; Bruce, P. G. *Nature* **2001**, *412*, 520−523.
(21) Vachon, C.; Vasco, M.; Perrier, M.; Prud'homme', J. *Macromolecules* **1993**, *26*, 4023−4031.
(22) Bergman, R.; Börjesson, L.; Fytas, G.; Torell, L. M. *J. Non-Cryst. Solids* **1994**, *172−174* (Part 2), 830−837.
(23) Vachon, C.; Labreche, C.; Vallee, A.; Besner, S.; Dumont, M.; Prud'homme, J. *Macromolecules* **1995**, *28*, 5585−5594.
(24) Zhang, S.; Runt, J. *J. Phys. Chem. B* **2004**, *108*, 6295−6302.
(25) Wang, Y.; Agapov, A. L.; Fan, F.; Hong, K.; Yu, X.; Mays, J.; Sokolov, A. P. *Phys. Rev. Lett.* **2012**, *108*, 088303.
(26) Gainaru, C.; Hiller, W.; Bohmer, R. *Macromolecules* **2010**, *43*, 1907−1914.
(27) Ferry, A. *J. Phys. Chem. B* **1997**, *101*, 150−157.
(28) Kaminski, K.; Kipnusu, W. K.; Adrjanowicz, K.; Mapesa, E. U.; Iacob, C.; Jasiurkowska, M.; Wlodarczyk, P.; Grzybowska, K.; Paluch, M.; Kremer, F. *Macromolecules* **2013**, *46*, 1973−1980.
(29) Andersson, S. P.; Andersson, O. *Macromolecules* **1998**, *31*, 2999−3006.
(30) Roland, C. M.; Psurek, T.; Pawlus, S.; Paluch, M. *J. Polym. Sci., Part B: Polym. Phys.* **2003**, *41*, 3047−3052.
(31) Roland, C. M.; Hensel-Bielowka, S.; Paluch, M.; Casalini, R. *Rep. Prog. Phys.* **2005**, *68*, 1405.
(32) Grzybowska, K.; Grzybowski, A.; Ziolo, J.; Paluch, M.; Capaccioli, S. *J. Chem. Phys.* **2006**, *125*, 044904.

(33) Grzybowska, K.; Grzybowski, A.; Ziolo, J.; Rzoska, S. J.; Paluch, M. *J. Phys.: Condens. Matter* **2007**, *19*, 376105.
(34) Fontanella, J. J. *J. Chem. Phys.* **1999**, *111*, 7103−7109.
(35) Bendler, J. T.; Fontanella, J. J.; Shlesinger, M. F. *Phys. Rev. Lett.* **2001**, *87*, 195503.
(36) Bendler, J. T.; Fontanella, J. J.; Shlesinger, M. F.; Wintersgill, M. C. *Electrochim. Acta* **2003**, *48*, 2267−2272.
(37) Kremer, F.; Schohals, A. *Broadband Dielectric Spectroscopy*; Springer-Verlag: Berlin, 2002.
(38) Wübbenhorst, M.; van Turnhout, J. *J. Non-Cryst. Solids* **2002**, *305*, 40−49.
(39) Schonhals, A.; Schlosser, E. *Prog. Colloid Polym. Sci.* **1993**, *91*, 158−161.
(40) Schüller, J.; Mel'nichenko, Y. B.; Richert, R.; Fischer, E. W. *Phys. Rev. Lett.* **1994**, *73*, 2224−2227.
(41) Schonhals, A.; Stauga, R. *J. Chem. Phys.* **1998**, *108*, 5130−5136.
(42) Hayakawa, T.; Adachi, K. *Polymer* **2001**, *42*, 1725−1732.
(43) Mattsson, J.; Bergman, R.; Jacobsson, P.; Börjesson, L. *Phys. Rev. Lett.* **2003**, *90*, 075702.
(44) Gainaru, C.; Bohmer, R. *Macromolecules* **2009**, *42*, 7616−7618.
(45) Paluch, M.; Pawlus, S.; Kaminski, K. *J. Chem. Phys.* **2011**, *134*, 037101.
(46) Richert, R.; Agapov, A.; Sokolov, A. P. *J. Chem. Phys.* **2011**, *134*, 104508.
(47) Fragiadakis, D.; Dou, S.; Colby, R. H.; Runt, J. *J. Chem. Phys.* **2009**, *130*, 064907.
(48) Bordi, F.; Cametti, C.; Colby, R. H. *J. Phys.: Condens. Matter* **2004**, *16*, R1423.
(49) Bergman, R.; Brodin, A.; Engberg, D.; Lu, Q.; Angell, C. A.; Torell, L. M. *Electrochim. Acta* **1995**, *40*, 2049−2055.
(50) Stolwijk, N. A.; Obeidi, S. *Phys. Rev. Lett.* **2004**, *93*, 125901.
(51) Engberg, D.; Schüller, J.; Strube, B.; Sokolov, A. P.; Torell, L. M. *Polymer* **1999**, *40*, 4755−4761.
(52) Bernson, A.; Lindgren, J. *Polymer* **1994**, *35*, 4848−4851.
(53) Rubinstein, M.; Colby, R. H. *Polymer Physics*; Oxford University Press: Oxford, U.K., 2003.
(54) Walden, P. *Z. Phys. Chem.* **1906**, *55*, 207−249.
(55) Xu, W.; Angell, C. A. *Science* **2003**, *302*, 422−425.
(56) Belieres, J.-P.; Angell, C. A. *J. Phys. Chem. B* **2007**, *111*, 4926−4937.
(57) Angell, C. A.; Ansari, Y.; Zhao, Z. *Faraday Discuss.* **2012**, *154*, 9−27.
(58) Lee, S.-Y.; Ueno, K.; Angell, C. A. *J. Phys. Chem. C* **2012**, *116*, 23915−23920.
(59) Wei, X.; Shriver, D. F. *Chem. Mater.* **1998**, *10*, 2307−2308.
(60) Ferry, A.; Edman, L.; Forsyth, M.; MacFarlane, D. R.; Sun, J. *J. Appl. Phys.* **1999**, *86*, 2346−2348.
(61) Ferry, A.; Edman, L.; Forsyth, M.; MacFarlane, D. R.; Sun, J. *Electrochim. Acta* **2000**, *45*, 1237−1242.
(62) Forsyth, M.; Jiazeng, S.; MacFarlane, D. R. *Electrochim. Acta* **2000**, *45*, 1249−1254.
(63) Imrie, C. T.; Ingram, M. D. *Electrochim. Acta* **2001**, *46*, 1413−1417.
(64) Agapov, A. L.; Sokolov, A. P. *Macromolecules* **2011**, *44*, 4410−4414.
(65) Ratner, M. A.; Shriver, D. F. *Chem. Rev.* **1988**, *88*, 109−124.
(66) Ratner, M. A.; Johansson, P.; Shriver, D. F. *MRS Bull.* **2000**, *25*, 31−37.